Ground-state magneto-optical resonances in cesium vapor confined in an extremely thin cell

C. Andreeva,[1] A. Atvars,[2] M. Auzinsh,[2] K. Blush,[2] S. Cartaleva,[1,*] L. Petrov,[1] and D. Slavov[1]
[1]*Institute of Electronics, Bulgarian Academy of Sciences, Boulevard Tzarigradsko shosse 72, 1784 Sofia, Bulgaria*
[2]*Department of Physics and Institute of Atomic Physics and Spectroscopy, University of Latvia, 19 Rainis Boulevard, LV-1586 Riga, Latvia*
(Received 22 April 2007; published 10 December 2007)

Experimental and theoretical studies are presented related to the ground-state magneto-optical resonance observed in cesium vapor confined in an extremely thin cell (ETC), with thickness equal to the wavelength of the irradiating light. It is shown that utilization of the ETC allows one to examine the formation of a magneto-optical resonance on the individual hyperfine transitions, thus distinguishing processes resulting in dark (reduced absorption) or bright (enhanced absorption) resonance formation. We report experimental evidence of bright magneto-optical resonance sign reversal in Cs atoms confined in an ETC. A theoretical model is proposed based on the optical Bloch equations that involves the elastic interaction processes of atoms in the ETC with its walls, resulting in depolarization of the Cs excited state, which is polarized by the exciting radiation. This depolarization leads to the sign reversal of the bright resonance. Using the proposed model, the magneto-optical resonance amplitude and width as a function of laser power are calculated and compared with the experimental ones. The numerical results are in good agreement with those of experiment.

DOI: 10.1103/PhysRevA.76.063804 PACS number(s): 42.50.Gy

I. INTRODUCTION

Recently, the high-resolution spectroscopy of alkali-metal atoms confined in a thin cell has proven very promising for studies not only of atom-light but also of atom-surface interactions [1]. The realization of such atomic layers has become possible through the development of so-called extremely thin cells (ETCs) whose distance between the windows is of the order of and less than 1 μm. Thus, the ETC confines a thin gas layer with a thickness of less than 1 μm and typical diameters of a few centimeters [2]. This causes a strong anisotropy in the atom-light interaction, which leads to two main effects in the observed absorption and fluorescence spectra, and makes these spectra different from those obtained in ordinary (centimeter-sized) cells. First, most of the atoms with a velocity component normal to the cell walls collide with the walls before completing the absorption-fluorescence cycle with the incoming light. Hence, these atoms give a smaller contribution to the atomic fluorescence compared to atoms flying parallel to the cell walls. Since generally the light propagation direction is perpendicular to the cell windows, the Doppler broadening of the optical transitions between various levels of the hyperfine structure (hfs), noted for simplicity further as hfs transitions, is significantly reduced. Thus, the hfs transitions, which are strongly overlapped in ordinary (centimeter-sized) cells, in the ETC are well resolved with single-beam spectroscopy. Unlike in saturation spectroscopy, the sub-Doppler absorption in an ETC is linear up to relatively large laser power densities, which allows, for example, the determination of transition probabilities of the different hfs transitions [3]. The absence of crossover resonances can also be advantageous when investigating more complex spectra.

Second, the investigation of atoms confined in cells whose thickness L is comparable to the wavelength of the light, λ, leads to the observation of interesting coherent effects. It has been shown that the width of the hfs transitions in absorption changes periodically with cell width, with minima at $L=(2n+1)\lambda/2$ [4], because of the realization of the Dicke regime [5] in the optical domain. Moreover, for the ETC a significant difference between the absorption and fluorescence spectra can be observed because the faster atoms with sufficient interaction time for the absorption of a photon, but not enough for its subsequent release, will contribute to the absorption signal but not to the fluorescence signal [2,6].

Coherent population trapping (CPT) resonances prepared in the Hanle configuration have been widely investigated for Cs and Rb atoms confined in ordinary cells. The alkali-metal atoms are situated in the magnetic field $\mathbf{B}$ with time-dependent variations around $\mathbf{B}=\mathbf{0}$. At the same time they are irradiated by a monochromatic laser field in such a configuration that different polarization components of the light couple the atomic Zeeman sublevels of one of the ground-state hfs levels through a common excited one, and introduce coherence between ground magnetic sublevels at $\mathbf{B}=\mathbf{0}$. The applied magnetic field $\mathbf{B}$ is oriented in a direction orthogonal to the atomic orientation and alignment produced by the light. As has been shown in [7–12], for degenerate two-level systems in the absence of depolarizing collisions of the excited state, two types of resonance can be observed, depending on the ratio of the degeneracies of the two states involved in the optical transition: electromagnetically induced transparency (EIT, dark magneto-optical) resonance or electromagnetically induced absorption (EIA, bright magneto-optical) resonance. The EIT resonance is realized when the condition $F_g \rightarrow F_e = F_g - 1, F_g$ is met, while the EIA resonance is observed for the $F_g \rightarrow F_e = F_g + 1$ type of transitions. Here, F_g and F_e are the hfs quantum numbers of the ground- and excited-state hfs levels, respectively.

The significant disadvantage of magneto-optical resonance studies in ordinary cells is that, because of the Doppler

*stefka-c@ie.bas.bg

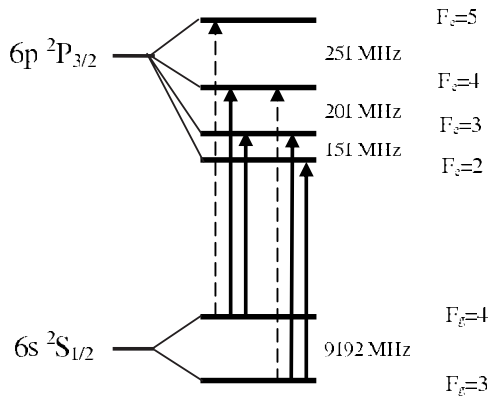

FIG. 1. Energy-level diagram for the D_2 line of ^{133}Cs. $F_g \rightarrow F_e \leq F_g$ transitions (solid line) are distinguished from $F_g \rightarrow F_e > F_g$ transitions (dashed line).

broadening in thermal cells, a strong overlapping takes place between hfs transitions responsible for dark and bright resonances. Therefore, it is important to make use of the fact that in an ETC the hyperfine transitions are well resolved, and the coherent effects can be investigated under better-defined conditions than in the case of ordinary cells. Moreover, the possibility of separating the contributions of slow and fast atoms to the magneto-optical signal, provided by using the ETC, will result in a better understanding of the transient processes in the formation of the coherent resonances. In addition, magneto-optical resonance investigations in ETCs could give information about the influence of the cell walls on the atomic polarization, because the main contribution to the magneto-optical signal is expected from the atoms flying "a long way" along the cell window.

In this work, we present experimental and theoretical results concerning the ground-state magneto-optical resonances on the D_2 line of Cs, obtained at the individual hfs transitions starting from F_g=3 and 4. It is shown that, in the ETC (with thickness equal to the light wavelength), dark (reduced absorption) magneto-optical resonances are observed at $F_g \rightarrow F_e = F_g - 1, F_g$ transitions, which are similar to the results obtained in ordinary cells. A very interesting result is obtained at $F_g \rightarrow F_e = F_g + 1$ transitions. For these transitions, we demonstrate here that the bright (enhanced absorption) resonance registered in ordinary cells in the case of an ETC is reversed into a dark one. This effect is attributed to the depolarization of the Cs atoms' excited levels due to elastic collisions with the ETC walls. A theoretical model has been developed based on the optical Bloch equations and involving the elastic interaction processes of atoms in an ETC with walls that affect the polarization of the atomic excited levels. The numerical results are in good qualitative agreement with the experimental ones.

II. CESIUM ENERGY LEVELS AND EXPERIMENTAL SETUP

The relevant Cs energy levels and hfs transitions involved are illustrated in Fig. 1. The two groups of allowed hfs transitions (starting from F_g=3 and 4) are denoted. The hfs transitions responsible for the formation of dark or bright magneto-optical resonances are denoted by solid or dashed lines, respectively. It should be noted that the Doppler broadening of the optical hfs transitions in an ordinary cell (~400 MHz) is larger than the separation between the excited-state hfs levels. As a result, in the ordinary cell the profiles of the three hfs transitions starting from a single ground hfs level strongly overlap and form a single absorption (fluorescence) line. Hence, the three different types of hfs transitions, responsible for the formation of both dark and bright resonances, are involved in a single fluorescence line.

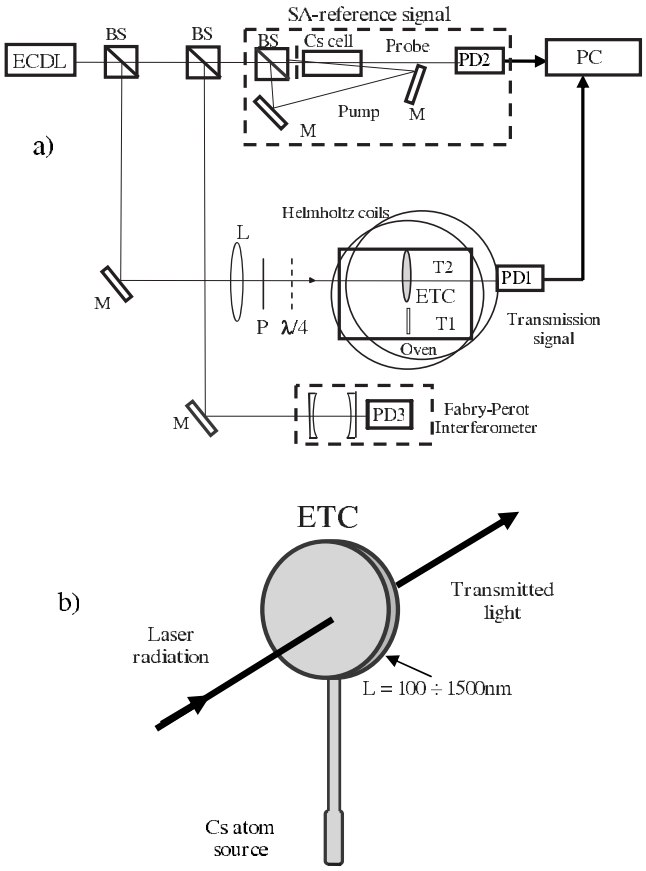

FIG. 2. Experimental setup (a) and sketch of ETC (b).

In the case of monomode laser excitation of dilute Cs vapor (without velocity-changing collisions between atoms) contained in an ordinary cell [12], the three hfs transitions forming the fluorescence line will be excited independently, each one at a different velocity class of atoms. Under these conditions, the open transitions are depleted because of the optical pumping to the ground hfs level, which does not interact with the laser light. Therefore, they do not play a significant role in the formation of the magneto-optical resonance. Thus, the sign of the magneto-optical resonance is mainly determined by the closed transition, which does not suffer hfs optical pumping. As a result, in the ordinary cells dark resonances are observed at the fluorescence line starting from F_g=3 and bright resonances at the fluorescence line starting from the F_g=4 levels. The dark resonance observed on the fluorescence line starting from F_g=3 has been attrib-

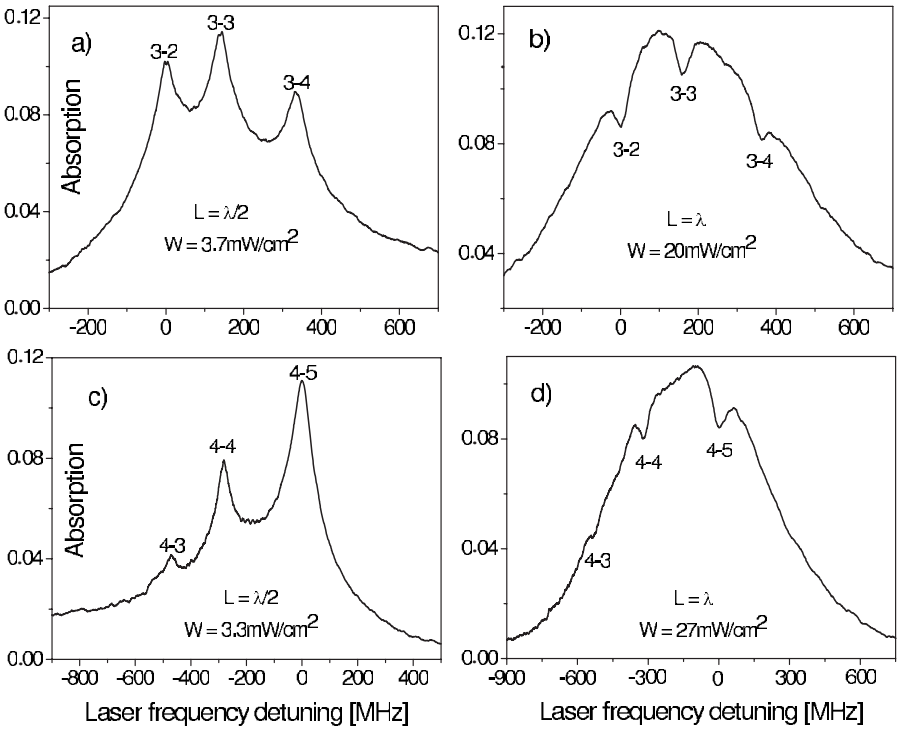

FIG. 3. Absorption spectra at $F_g=3$ (a), (b) and 4 (c), (d) sets of hf transitions, for ETC thickness $L=\lambda/2$ (a), (c) and λ (b), (d).

uted to the contribution of the $F_g=3\rightarrow F_e=2$ closed transition, while the bright resonance is related to the $F_g=4\rightarrow F_e=5$ closed transition.

The experimental setup used is schematically presented in Fig. 2(a). A cw extended cavity diode laser (ECDL) was used as the radiation source. It was operated in single-frequency mode with $\lambda=852$ nm and linewidth of about 3 MHz. Thus, because of the narrow bandwidth of the laser, it was possible to excite separately the different hfs transitions of the D_2 line of ^{133}Cs atoms $[6S_{1/2}(F_g=3)\rightarrow 6P_{3/2}(F_e=2,3,4)$ or $6S_{1/2}(F_g=4)\rightarrow 6P_{3/2}(F_e=3,4,5)]$. The main part of the laser beam was directed at normal incidence onto the ETC [zoomed in Fig. 2(b)] with a source containing Cs. The ETC operates with a specially constructed oven which maintains a constant temperature gradient between the Cs atom source (temperature T_1) and the cell windows (temperature T_2), $T_2>T_1$. The Cs vapor density is controlled by changing the source temperature. The ETC is placed between a pair of coils in Helmholtz configuration, which allows application of magnetic field **B** varied around $\mathbf{B}=0$ and oriented in a direction orthogonal to the laser beam propagation direction. No shielding against stray laboratory magnetic fields B_{str} (of about 0.5 G) is provided. The light transmitted through the ETC is measured by photodiode PD1.

Most of the experiments were performed by irradiating Cs atoms by means of linearly polarized light. In this case the varied magnetic field **B** is orthogonal both to the laser beam and to the light polarization. When light with circular polarization is used, a quarter-wave plate is inserted before the ETC, after the polarizer P.

First, an experiment was performed, aimed at general observation of the magneto-optical resonance amplitude and sign along the entire absorption line profile. In this case, the laser frequency was scanned over the absorption profile with a rate of about two orders of magnitude less than that of the magnetic field variation around $\mathbf{B}=0$. This double-scanning technique, introduced in [12], is discussed in more detail in Sec. IV. During the second part of the experiment related to the magneto-optical resonance study, the light frequency was fixed at the center of the examined hfs transition and Cs atom absorption was measured as a function of the magnetic field **B**.

The remaining part of the laser beam was separated into two parts and was used for laser frequency control: one part was sent to a scanning Fabry-Pérot interferometer in order to monitor the single-mode operation of the ECDL, and the second one to an additional branch of the setup including an ordinary, 3-cm-long Cs cell, for simultaneous registration of the saturated absorption (SA) spectrum. The latter was used for precise scaling and reference of the laser frequency. In addition (see Sec. V), the ordinary cell was used for monitoring of the magneto-optical resonances in the probe beam absorption. In this way, the $\mathbf{B}=\mathbf{0}$ points can be determined experimentally during the performed double scan of laser frequency and magnetic field **B** (see Sec. IV).

III. ABSORPTION SPECTRA AT THE ETC THICKNESS $L=\lambda/2$ AND $L=\lambda$

In order to help further the discussion related to magneto-optical resonances observed in the ETC, in this section we present the absorption spectra of both absorption lines at two thicknesses of the ETC (Fig. 3), observed at $\mathbf{B}=\mathbf{0}$ (i.e., under the influence of the weak B_{str} only). For $L=\lambda/2$, the absorption spectra of the lines starting from $F_g=3$ and 4 are illustrated in Figs. 3(a) and 3(c). It can be seen that the spectral profiles of all hfs transitions are well resolved due to the significant enhancement of atomic absorption at the hfs transition center and its reduction toward the wings. As was mentioned in the Introduction, the origin of the narrowing of

the hfs transition profiles is attributed to the Dicke effect. The processes responsible for the coherent Dicke narrowing of the hfs transition profile at $L=\lambda/2$ can be briefly summarized as follows [4,6,13]. If an atom at the moment of leaving the cell wall is excited by resonant light, the excitation will start to precess in phase with the exciting electromagnetic field at the wall position. However, with the atomic motion the excitation will drift gradually out of phase with the local exciting field. The phase mismatch appearing on the line center under a weak exciting field is independent of the atomic velocity and, for a cell thickness up to $\lambda/2$, all regions of the cell interfere constructively, leading to a strong absorption enhancement at the hfs transition center. However, if the exciting light is detuned from the hfs transition center, the angular precession of the atomic excitation becomes velocity dependent, resulting in a smooth reduction of the absorption in the wings of the profile.

Unlike the atomic spectra observed at $L=\lambda/2$, when the cell thickness rises up to $L=\lambda$, a completely different behavior of the transition absorption occurs [Figs. 3(b) and 3(d)]. Under this condition, the Dicke narrowing vanishes and at low light power density the Doppler profiles of hfs transitions forming the absorption line are completely overlapped. However, starting from a power density W of several $\mathrm{mW/cm^2}$, narrow dips of reduced absorption occur, centered at each hfs transition. The observed dips are attributed to velocity-selective saturation of the hfs transition and to velocity-selective population loss due to optical pumping to the ground-state level that does not interact with the exciting light field. To complete the saturation and/or optical pumping process, the atom needs a longer interaction time with the exciting light than for the single act of absorption [14]. Due to this, primarily the very slow atoms or those flying parallel to the ETC windows can contribute to the reduced absorption dips at $L=\lambda$. Note that it is expected that the latter group of atoms will be responsible for magneto-optical resonance formation, because this process is also slower than ordinary linear absorption.

IV. DOUBLE LASER FREQUENCY AND MAGNETIC FIELD SCANNING

As shown in the previous section, an important advantage of using the ETC is that it is possible to study the absorption behavior of the individual hfs transitions. In order to use this advantage for the magneto-optical resonance study, the following experiment is performed. The laser frequency is slowly scanned over the hfs transition profile. During this slow scan, the magnetic field is varied around $\mathbf{B}=\mathbf{0}$ with a frequency about two orders of magnitude higher than the frequency of the laser scan. Such a double-scan method was proposed in Ref. [12], and it allows the observation of a sequence of magneto-optical resonances superimposed on the absorption profile of the transition, registered during the laser frequency detuning. For the dark resonance, the minimum absorption should be observed at $\mathbf{B}=\mathbf{0}$, while it is opposite for the bright one: the maximum absorption is at $\mathbf{B}=\mathbf{0}$. This technique is illustrated in Fig. 4, for the absorption line starting from the $F_g=4$ level on the D_2 line of Cs atoms

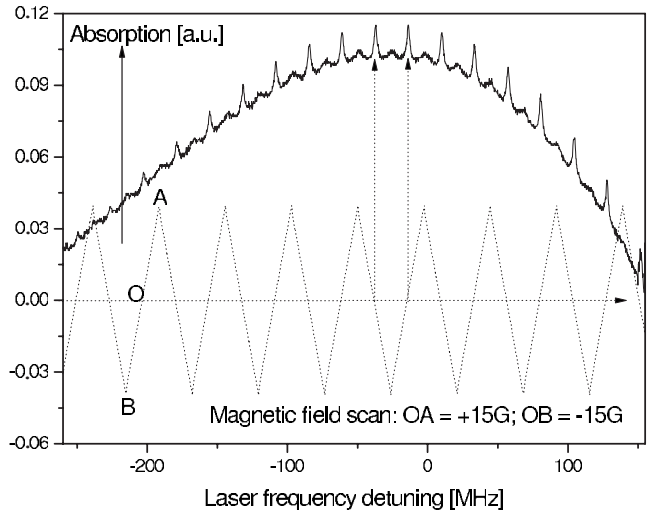

FIG. 4. Illustration of the double laser frequency–magnetic field scanning approach, in the case of an ordinary cell at room temperature (20 °C). Laser frequency detuning is denoted starting from the $F_g=4 \rightarrow F_e=5$ transition. The bright magneto-optical resonances are superimposed on the absorption profile of the $F_g=4$ set of transitions (solid line). For monitoring of the $\mathbf{B}=\mathbf{0}$ positions, the simultaneous magnetic field variations are also shown (dotted line). Cs atoms are irradiated by circularly polarized laser light.

contained in an ordinary cell. From the figure, it can be seen that a number of bright magneto-optical resonances are superimposed on the Cs absorption profile. Note that the bright resonances are observed over the entire absorption line. The width and separation of these resonances depend on the ratio of the laser frequency and the magnetic field scanning rates, as well as on the value of the magnetic field variation. Hence, this approach cannot be used for characterization of the magneto-optical resonance profile. However, at each laser frequency detuning, the resonance sign (bright or dark) can be unambiguously determined.

V. MAGNETO-OPTICAL RESONANCE OBSERVATION IN AN ETC WITH THICKNESS $L=\lambda$: THE BRIGHT RESONANCE SIGN REVERSAL

The approach briefly described in the previous section is applied for investigation of the magneto-optical resonances in an ETC. First, the magneto-optical resonances at the three hfs transitions starting from the $F_g=3$ level are examined (Fig. 5). For precise monitoring of the $\mathbf{B}=\mathbf{0}$ points during the double scan used, magneto-optical resonances are simultaneously registered in the probe beam of the ordinary cell used for SA resonance observation (Fig. 5, dashed lines). The ordinary cell is situated outside the Helmholtz coils, so the magnetic field from the Helmholtz coils there is not homogeneous and its value is lower than that applied to the ETC. Hence, it is not possible to compare the widths of magneto-optical resonances observed in both cells but the determination of the $\mathbf{B}=\mathbf{0}$ points, which are the minima of the dark resonances in the ordinary cell, is correct. The magneto-optical resonances in the ordinary cell are registered only for determination of the $\mathbf{B}=\mathbf{0}$ points. As shown in Ref. [12], in

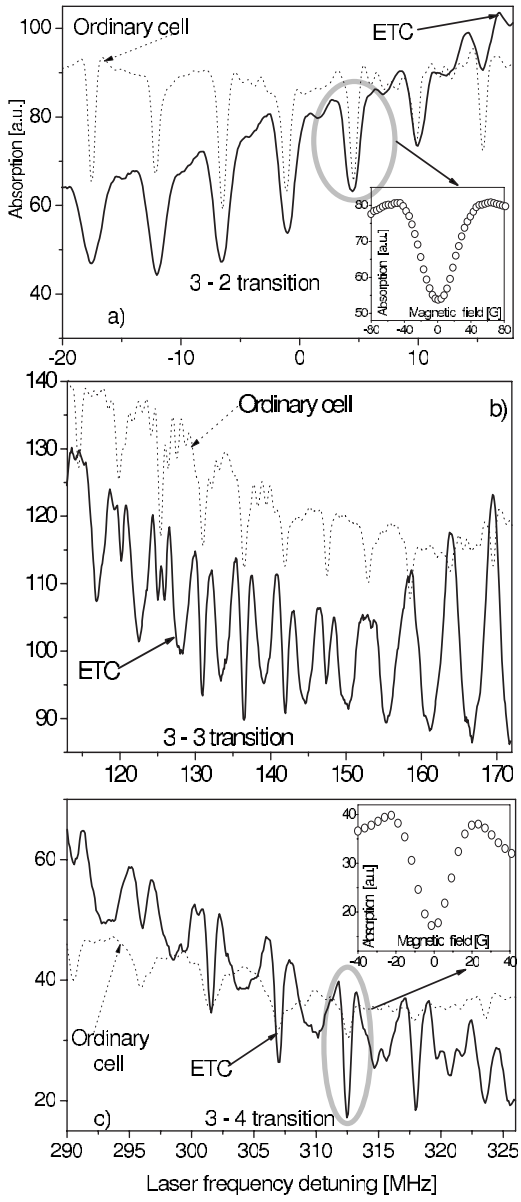

FIG. 5. Magneto-optical resonances superimposed on the ETC absorption (solid line) obtained by laser frequency detuning in small intervals around the centers of $F_g=3\rightarrow F_e=2$ (a) (inset: illustration of single magneto-optical resonance), $F_g=3\rightarrow F_e=3$ (b), and $F_g=3\rightarrow F_e=4$ (c) (inset: dark resonance at the intrinsically bright transition) transitions. For monitoring of the $F_g=3$ positions, a simultaneous recording of the resonances in the absorption of the ordinary cell is shown (dashed line). Cs source temperature is 120 °C, ETC thickness $L=\lambda$, and laser power $W=66$ mW/cm^2. Cs atoms are irradiated by linearly polarized laser light.

the case of an ordinary cell, dark resonances are observed at the $F_g=3$ absorption line.

Figure 5(a) illustrates the fact that magneto-optical dark resonances are observed in a frequency region of a few tens of megahertz around the $F_g=3\rightarrow F_e=2$ transition center. This interval is significantly narrower than the Doppler width of the corresponding hfs transition. The resonance profile as a function of magnetic field **B** is illustrated in the inset of Fig. 5(a). The sign of the magneto-optical resonance observed in the ETC corresponds to that observed in an ordinary cell. A dark resonance is observed at the $F_g=3\rightarrow F_e=3$ transition [Fig. 5(b)], and it also exists in a narrow region around the hfs transition center. For this transition, the resonance sign is also in agreement with the observations in ordinary cells. From Fig. 5(b) it can be seen that the dark resonance (with minimum absorption at $\mathbf{B}=\mathbf{0}$) observed for slow atoms is superimposed on another feature having maximum absorption at $\mathbf{B}=\mathbf{0}$. Three full profiles of this type of feature can be seen in Fig. 5(b) for laser frequency detuning in the interval of 155–170 MHz. They are clearly observed for atoms with velocity higher than that of slow atoms having Doppler shift within the homogeneous width around the center of the hfs transition. This type of Cs absorption dependence on the magnetic field, which is broader than the dark resonance, has a maximum at $\mathbf{B}=\mathbf{0}$, and is not related to the coherent superposition of atomic levels, will be discussed in more detail later in this section.

As mentioned in the Introduction, bright resonances are observed at $F_g\rightarrow F_e=F_g+1$ transitions of dilute alkali-metal atoms contained in the ordinary cells, where the collisions between atoms can be neglected. Due to this, in the ETC, a narrow bright resonance was expected for the $F_g=3\rightarrow F_e=4$ transition. However, at the intrinsically bright $F_g=3\rightarrow F_e=4$ transition, a dark resonance is observed in the ETC [Fig. 5(c)]. As can also be seen from the inset of Fig. 5(c), the absorption (at the $F_g=3\rightarrow F_e=4$ transition) as a function of magnetic field **B** shows a dark resonance. Hence we demonstrate that in the dilute vapor confined by the ETC the bright resonance sign is reversed to a dark one. It should be pointed out that the $F_g=3\rightarrow F_e=4$ transition is an open one, with a transition probability significantly less than that of the closed $F_g=3\rightarrow F_e=2$ transition. As a result, in the ordinary cell it was not possible to observe the magneto-optical resonances determined by this transition.

In order to obtain more information about the behavior of the $F_g\rightarrow F_e=F_g+1$ type of transitions in the ETC, the $F_g=4$ set of transitions was investigated, where the $F_g=4\rightarrow F_e=5$ transition is closed and has the highest probability. The results obtained are presented in Fig. 6 where only the ETC signal is shown (in the presence and in the absence of the magnetic field B). In the first case (Fig. 6, solid line), the $\mathbf{B}=\mathbf{0}$ points are not noted and we will specify the magneto-optical resonance sign. At low light power [Fig. 6(a)], the above-mentioned broader features predominate over the whole region of the presented absorption spectrum, including the central regions of the three hfs transitions. At the centers of the hfs transitions, only very small-amplitude dark magneto-optical resonances are observed, superimposed on the tops of the profiles having maxima at $\mathbf{B}=\mathbf{0}$. When increasing the light power [Fig. 6(b)], the dark resonance amplitude increases and, as in the case of the $F_g=3$ set of transitions, they are observed in a narrow interval around the center of the hfs transitions. More specifically, the magneto-optical resonances are observed only within the frequency intervals where the reduced absorption dips occur in the Cs absorption spectrum at $L=\lambda$ (Fig. 6, dashed curve obtained at $\mathbf{B}=\mathbf{0}$). Hence, only slow atoms within the homogeneous linewidth contribute to the formation of the magneto-optical resonance.

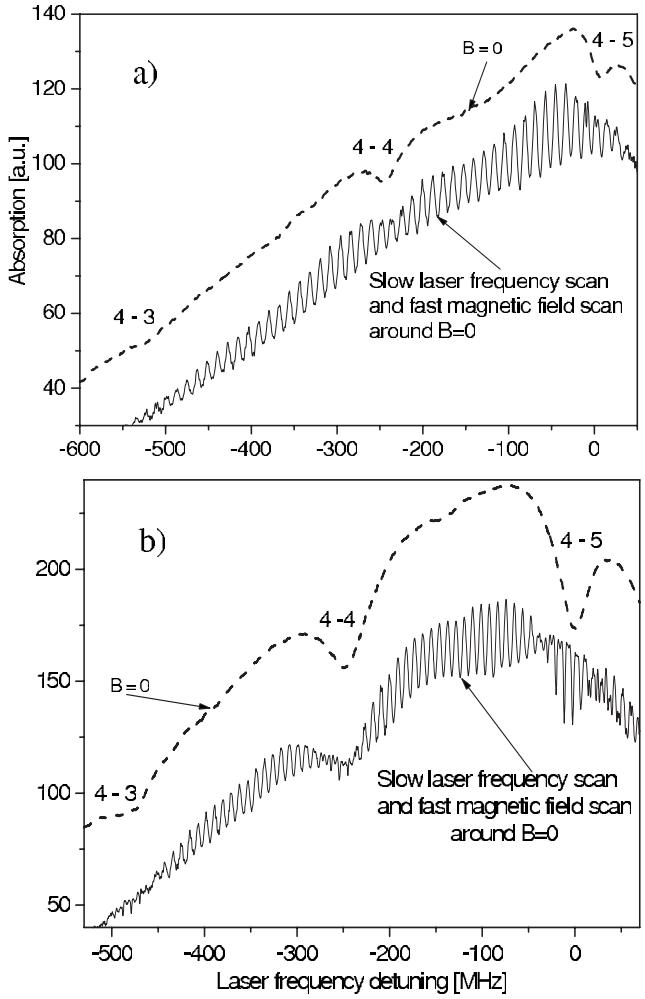

FIG. 6. Magneto-optical resonances superimposed on the ETC absorption spectrum (solid line) and the corresponding part of the ETC absorption spectrum (dashed line) at the $F_g=4$ absorption line for two different laser powers $W=13$ (a) and 133 mW/cm^2 (b). Cs source temperature is 131 °C, $L=\lambda$, linearly polarized laser light.

In the remaining regions of the light frequency scan, only the above-mentioned features, which are assumed to be of noncoherent origin, are observed. Our experiment has shown that, for very low laser power, these features are observed over the entire absorption spectra of both $F_g=3,4$ sets of transitions. Hence, the discussed features appear under conditions sufficient for the realization of a single event of absorption. As the formation of the magneto-optical resonance requires alignment and orientation of atoms (including several absorption-fluorescence cycles), which is a much longer process, we believe that the formation of the noncoherent feature is related to the large magnetic field scan (−90 G, +90 G) needed to register the magneto-optical resonance. To understand this effect, suppose that the laser light is in resonance with a certain velocity class of atoms. As the width of the irradiating light is small (3 MHz), only at $B=0$ will all transitions starting from different Zeeman sublevels be in exact resonance with the laser light. Taking into consideration the Zeeman splitting of the ground-state levels (0.35 MHz/G) and the excited state (0.93 MHz/G for $F_e=2$, 0.00 for $F_e=3$, 0.37 MHz/G for $F_e=4$, 0.56 MHz/G for $F_e=5$), it can be estimated that the magnetic field increase will significantly shift from the laser light frequency the centers of the optical transitions starting from different ground-state Zeeman sublevels. These shifts will be proportional to the m_F value, and only the $m_{F_g}=0\rightarrow m_{F_e}=0$ transitions will stay in resonance with the laser light during the magnetic field scan.

In general, the shifts of centers of the different transitions are significant compared to their natural width and might be considered as a reason for the reduced absorption of the Cs atom when the magnetic field is detuned from zero value. Thus features are formed in the absorption dependence on magnetic field, with maxima at $\mathbf{B=0}$. To summarize, we attribute the discussed features to the noncoherent dependence of the absorption on the magnetic field, whose origin are the shifts of the Zeeman transition centers from the light frequency with the magnetic field scan. Hence, only slow atoms, which have time enough to suffer optical pumping and saturation, are involved in the formation of the magneto-optical resonances. Fast atoms, which have much shorter interaction time with the light, are mainly responsible for the appearance of the noncoherent feature.

Figure 7 illustrates the dependence of the magneto-optical resonance [Figs. 7(a) and 7(b)] and the noncoherent feature [Fig. 7(c)] on magnetic field. The dark magneto-optical resonance that is observed for slow atoms at all $F_g\rightarrow F_e=F_g-1,F_g$ transitions is illustrated in Fig. 7(a), for the closed

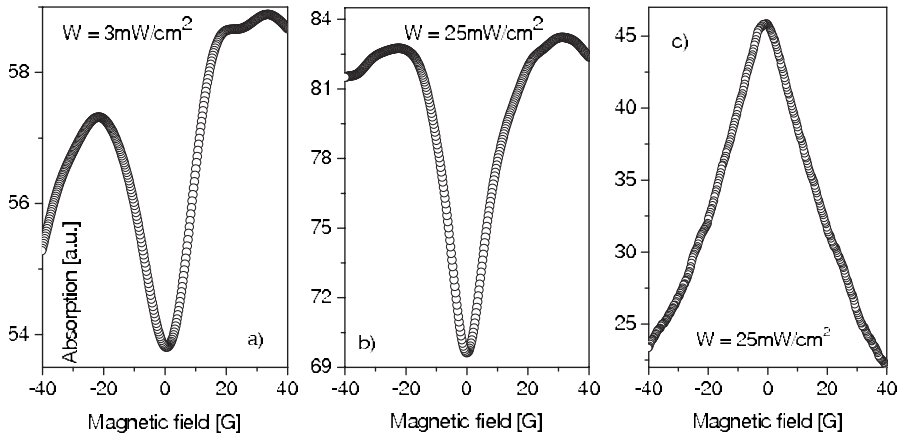

FIG. 7. Illustration of dark magneto-optical resonances observed at $F_g=3\rightarrow F_e=2$ (a) and 4 (b) transitions for slow atoms, and noncoherent feature (c) observed for fast atoms. Cs source temperature is 112 °C and $L=\lambda$.

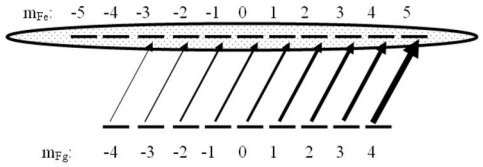

FIG. 8. Illustration of the transformation of bright to dark resonance at the $F_g=4\rightarrow F_e=5$ transition, in the case of depolarizing $F_e=5$ level collisions between Cs and buffer gas atoms.

$F_g=3\rightarrow F_e=2$ transition. In Fig. 7(b), the dark magneto-optical resonance that is observed in the case of slow atoms at the $F_g=3\rightarrow F_e=4$ transition is shown. The case of fast atoms is illustrated in Fig. 7(c). Similar results are observed by irradiating Cs atoms with circularly polarized light and applying a magnetic field orthogonal to the laser beam.

Coming back to Fig. 6(b), it should be particularly stressed that for the closed $F_g=4\rightarrow F_e=5$ transition a dark resonance is also evidenced in the case of the ETC. This result is very interesting, because precisely for this transition a very well-resolved bright resonance is observed in the ordinary cell containing dilute Cs atoms [12] (see also Fig. 4). However, it turns out that the bright resonance is very sensitive to the buffering of the ordinary cell. It has been found [12] and very recently confirmed [15,16] that if a cell containing alkali-metal atoms is buffered by some noble gas, the magneto-optical resonance at the $F_g=4\rightarrow F_e=5$ transition is changed from a bright to a dark one. Theoretical modeling has shown that this transformation of the resonance sign can be attributed to the depolarization of the F_e level by collisions of alkali-metal atoms with the buffer gas atoms. At the same time, these collisions do not lead to depolarization of the F_g level, thus preserving the coherent superposition of the ground-state magnetic sublevels introduced by the light at $\mathbf{B}=\mathbf{0}$. Note that the ordinary cell buffering does not reverse the sign of the dark magneto-optical resonances observed on the $F_g\rightarrow F_e=F_g-1,F_g$ type of transition.

To easily picture the physical processes that lead to the magneto-optical resonance sign reversal due to collisions between alkali-metal and buffer gas atoms in the ordinary cell, it is better to consider Cs atoms irradiated by circularly polarized light. In this case, the magneto-optical resonance is observed in absorption (fluorescence) as a function of the magnetic field orthogonal to the laser beam and scanned around $\mathbf{B}=\mathbf{0}$. Let us consider the $F_g=4\rightarrow F_e=5$ transition on the D_2 line of Cs (Fig. 8). In the absence of depolarizing collisions and in the presence of circularly polarized light (σ^+), because the Clebsch-Gordan coefficients increase for transitions starting from $m_{F_g}=-4$ to $m_{F_g}=4$, most atoms will circulate on the $m_{F_g}=4\rightarrow m_{F_e}=5$ transition, which is the transition with the highest probability of absorption for σ^+ polarization. Therefore, at $\mathbf{B}=\mathbf{0}$ a maximum in the absorption (fluorescence) will be observed. In the presence of a magnetic field perpendicular to the atomic orientation, part of the population of the $m_{F_g}=4$ sublevel will be redistributed to the other sublevels and the absorption (fluorescence) will be decreased, which results in the observation of a narrow resonance of enhanced absorption (fluorescence) determined as a bright magneto-optical resonance. However, if a buffer gas is added, a large fraction of the atoms accumulated on the $m_{F_e}=5$ sublevel will be redistributed among the other Zeeman sublevels of the $F_e=5$ level because of the depolarizing collisions between Cs and buffer gas atoms. Taking into account the difference in the probabilities of the transitions between the different Zeeman sublevels, it has been shown [12] that this redistribution leads to an accumulation (at $\mathbf{B}=\mathbf{0}$) of many atoms on the $m_{F_g}=-4$ sublevel, having the lowest probability for σ^+ excitation. Thus, the bright resonance observed in pure and dilute Cs vapor transforms into a dark one when buffer gas is added to the ordinary cell.

In analyzing the results related to the bright resonance sign reversal due to the depolarization of the excited state, an assumption has been made that in the ETC a similar depolarization of the excited state can occur due to the long-range interaction between alkali-metal atoms and the two window surfaces of the ETC. In support of this assumption, note that, during their interaction with the light, atoms responsible for the magneto-optical resonance formation fly a long way (on the order of a millimeter) along the ETC windows, which are separated only by a tiny gap very close to 852 nm. In fact, our experiment shows that only atoms within the homogeneous width of the hfs transition contribute to the magneto-optical resonance formation. Hence, the velocity selection of atoms forming the coherent resonance is much stronger than that of atoms participating in the ETC absorption events. As an additional support to the assumption related to the depolarization of the excited state, we report here the results of our measurement of the polarization of the fluorescence collected in a direction orthogonal to the laser beam. While in an ordinary cell containing dilute Cs vapor we measured a degree of fluorescence polarization $P=0.24$, in the ETC significant depolarization of the fluorescence was observed, yielding $P=0.02$. A theoretical model has been developed to analyze the experimental observations that will be presented in the following section.

VI. THEORETICAL MODEL

A. Introduction and definitions

We consider the dipole interaction of an atom with a laser field in the presence of an external static magnetic field $\mathbf{B}$. We assume that the atomic center of mass moves classically, which means that the only effect of the dipole interaction of the atom with the laser field is an excitation of a classically moving atom at the internal transitions. In this case the internal atomic dynamics is described by the semiclassical atomic density matrix ρ, which parametrically depends on the classical coordinates of the atomic center of mass.

We are interested in the optical Bloch equations (OBEs) for the density matrix elements $\rho_{g_ig_j}$, $\rho_{g_ie_j}$, $\rho_{e_ig_j}$, and $\rho_{e_ie_j}$, where g_i and g_j label atomic ground-state magnetic sublevels, and e_i and e_j excited-state magnetic sublevels. In writing the OBEs (see, for example, [17]),

$$\imath\hbar\frac{\partial\rho}{\partial t}=[\hat{H},\rho]+\imath\hbar\hat{R}\rho, \tag{1}$$

we consider the relaxation $\hat{R}$ due to spontaneous emission, transit relaxation, and interaction of atoms with the cell

walls—in both nonelastic and elastic collisions. We also assume that different velocity groups do not mix in atom-atom or atom-wall interactions, since the atomic density is sufficiently low (experiments are performed in dilute Cs vapor).

The Hamiltonian

$$\hat{H} = \widehat{H_0} + \widehat{H_B} + \hat{V} \tag{2}$$

includes the unperturbed atomic Hamiltonian $\widehat{H_0}$, which depends on the internal atomic coordinates: $\widehat{H_0}|\Psi_n\rangle = E_n|\Psi_n\rangle$, $\widehat{H_B}$ is the interaction of an atom with the external magnetic field $\mathbf{B}$, and $\hat{V} = -\hat{\mathbf{d}}\cdot\mathbf{E}(t)$ is the dipole interaction operator, where $\hat{\mathbf{d}}$ is the electric dipole operator. The exciting light is described classically by a fluctuating electric field $\varepsilon(t)$ of definite polarization $\mathbf{e}$:

$$\mathbf{E}(t) = \varepsilon(t)\mathbf{e} + \varepsilon^*(t)\mathbf{e}^*, \tag{3}$$

$$\varepsilon(t) = |\varepsilon_{\bar{\omega}}| e^{-\imath\Phi(t) - \imath(\bar{\omega} - \mathbf{k}_{\bar{\omega}}\mathbf{v})t} \tag{4}$$

with the center frequency of the spectrum $\bar{\omega}$ and the fluctuating phase $\Phi(t)$, which gives the spectrum a finite bandwidth $\Delta\omega$. The line shape of the exciting light is Lorentzian with full width at half maximum (FWHM) $\Delta\omega$.

B. Optical Bloch equations

Writing the OBEs explicitly for the density matrix element ρ_{ij}, we get

$$\begin{aligned}
\frac{\partial\rho_{ij}}{\partial t} &= -\frac{\imath}{\hbar}[\hat{H}, \rho_{ij}] + \hat{R}\rho_{ij} \\
&= -\frac{\imath}{\hbar}[\widehat{H_0}, \rho_{ij}] + \frac{\imath}{\hbar}[\hat{\mathbf{d}}\cdot\mathbf{E}(t), \rho_{ij}] + \hat{R}\rho_{ij} \\
&= -\imath\omega_{ij}\rho_{ij} + \frac{\imath}{\hbar}\mathbf{E}(t)\sum_k (\mathbf{d}_{ik}\cdot\rho_{kj} - \rho_{ik}\cdot\mathbf{d}_{kj}) + \hat{R}\rho_{ij} \\
&= -\imath\omega_{ij}\rho_{ij} + \frac{\imath}{\hbar}\varepsilon(t)\sum_k d_{ik}\rho_{kj} + \frac{\imath}{\hbar}\varepsilon^*(t)\sum_k d^*_{ik}\rho_{kj} \\
&\quad - \frac{\imath}{\hbar}\varepsilon(t)\sum_k d_{kj}\rho_{ik} - \frac{\imath}{\hbar}\varepsilon^*(t)\sum_k d^*_{kj}\rho_{ik} + \hat{R}\rho_{ij},
\end{aligned} \tag{5}$$

where $\omega_{ij} = (E_i - E_j)/\hbar$, and the transition dipole matrix elements $\mathbf{d}_{ij} = \langle i|\mathbf{d}|j\rangle$ and $d_{ij} = \langle i|\mathbf{d}\cdot\mathbf{e}|j\rangle$ can be calculated using the standard angular momentum algebra [18–20].

C. Simplification of the OBEs

Next, we apply the following procedure, which simplifies the OBEs. First, we use the rotating wave approximation [21]. After that we have stochastic differential equations [22] with stochastic variable $\partial\Phi(t)/\partial t$. In the experiment we measure time-averaged (stationary) values. Therefore, we need to perform the statistical averaging of the above equations. In order to do that, we solve the equations for the optical coherences and then take a formal statistical average over the fluctuating phases. We also apply the "decorrelation approximation" (which in general is valid only for Wiener-Levy-type phase fluctuations), allowing for separation of atom and field variables. With the decorrelation approximation, the small fluctuations of $\rho_{ij}(t)$ around its mean value $\langle\rho_{ij}(t)\rangle$ can be neglected. Finally, we assume a "phase diffusion" model for the description of the dynamics of the fluctuating phase. This model is usually used for description of the fluctuations of a single-mode laser with fluctuating phase. Thus we obtain a phase-averaged OBE. For a detailed description of the procedure of statistical averaging, the decorrelation approximation, Wiener-Levy-type phase fluctuations, and the phase-diffusion model, see [23] and references cited therein.

D. Steady-state excitation

Now we assume that atoms in the cell reach stationary excitation conditions (steady state). Under such conditions all density matrix elements in the OBEs become time independent. In these conditions we can eliminate the optical coherences $\rho_{g_ie_j}$ and $\rho_{e_ig_j}$ [14,17] from the OBEs. Thus, for the optical coherences we obtain the following explicit expressions:

$$\widetilde{\rho_{g_ie_j}} = \frac{\imath}{\hbar}\frac{|\varepsilon_{\bar{\omega}}|}{\Gamma_R + \imath\Delta_{e_jg_i}}\left(\sum_{e_k} d^*_{g_ie_k}\rho_{e_ke_j} - \sum_{g_k} d^*_{g_ke_j}\rho_{g_ig_k}\right), \tag{6}$$

$$\widetilde{\rho_{e_ig_j}} = \frac{\imath}{\hbar}\frac{|\varepsilon_{\bar{\omega}}|}{\Gamma_R - \imath\Delta_{e_ig_j}}\left(\sum_{g_k} d_{e_ig_k}\rho_{g_kg_j} - \sum_{e_k} d_{e_kg_j}\rho_{e_ie_k}\right), \tag{7}$$

where

$$\Delta_{ij} = \bar{\omega} - \mathbf{k}_{\bar{\omega}}\mathbf{v} - \omega_{ij} \tag{8}$$

and $\mathbf{k}_{\bar{\omega}}\mathbf{v}$ represents the Doppler shift of the transition energy of an atom due to its spatial motion. Here $\mathbf{k}$ is the wave vector of the excitation light and $\mathbf{v}$ is the atom velocity. In the present study it was assumed that in the ETC $\mathbf{k}_{\bar{\omega}}\mathbf{v} = 0$. Γ_R describes the effective relaxation,

$$\Gamma_R = \frac{\Gamma}{2} + \frac{\Delta\omega}{2} + \gamma + \Gamma_{col}, \tag{9}$$

where Γ is the spontaneous relaxation from level e, γ describes the relaxation rate, $\Delta\omega$ is the relaxation due to the finite linewidth of the laser (this relaxation is a consequence of the statistical averaging over the laser field fluctuations), and Γ_{col} describes the relaxation due to elastic atomic collisions with the cell walls.

E. Rate equations for Zeeman coherences

By substituting the expressions for the optical coherences, Eqs. (6) and (7), in the equations for the Zeeman coherences, we arrive at the rate equations for the Zeeman coherences only (see [23]):

$$\frac{\partial \rho_{g_i g_j}}{\partial t} = 0 = -\imath \omega_{g_i g_j} \rho_{g_i g_j} - \gamma \rho_{g_i g_j} + \sum_{e_i e_j} \Gamma^{e_i e_j}_{g_i g_j} \rho_{e_i e_j} + \lambda \delta(g_i, g_j) + \frac{|\varepsilon_{\bar{\omega}}|^2}{\hbar^2} \sum_{e_k, e_m} \left(\frac{1}{\Gamma_R + \imath \Delta_{e_m g_i}} + \frac{1}{\Gamma_R - \imath \Delta_{e_k g_j}} \right) d^*_{g_i e_k} d_{e_m g_j} \rho_{e_k e_m} - \frac{|\varepsilon_{\bar{\omega}}|^2}{\hbar^2} \sum_{e_k, g_m} \left(\frac{1}{\Gamma_R - \imath \Delta_{e_k g_j}} d^*_{g_i e_k} d_{e_k g_m} \rho_{g_m g_j} + \frac{1}{\Gamma_R + \imath \Delta_{e_k g_i}} d^*_{g_m e_k} d_{e_k g_j} \rho_{g_i g_m} \right), \tag{10}$$

$$\frac{\partial \rho_{e_i e_j}}{\partial t} = 0 = -\imath \omega_{e_i e_j} \rho_{e_i e_j} - \gamma \rho_{e_i e_j} - \Gamma \rho_{e_i e_j} - \Gamma_{col} \rho_{e_i e_j} + \Gamma_{col} \delta(e_i, e_j) \sum_{e_k} \frac{N_{e_k e_i}}{\sum_{e_m} N_{e_k e_m}} \rho_{e_k e_k} + \frac{|\varepsilon_{\bar{\omega}}|^2}{\hbar^2} \sum_{g_k, g_m} \left(\frac{1}{\Gamma_R - \imath \Delta_{e_i g_m}} + \frac{1}{\Gamma_R + \imath \Delta_{e_j g_k}} \right) d_{e_i g_k} d^*_{g_m e_j} \rho_{g_k g_m} - \frac{|\varepsilon_{\bar{\omega}}|^2}{\hbar^2} \sum_{g_k, e_m} \left(\frac{1}{\Gamma_R + \imath \Delta_{e_j g_k}} d_{e_i g_k} d^*_{g_k e_m} \rho_{e_m e_j} + \frac{1}{\Gamma_R - \imath \Delta_{e_i g_k}} d_{e_m g_k} d^*_{g_k e_j} \rho_{e_i e_m} \right). \tag{11}$$

Here $\Gamma^{e_i e_j}_{g_i g_j}$ describes the spontaneous relaxation from $\rho_{e_i e_j}$ to $\rho_{g_i g_j}$, λ describes the rate at which "fresh" atoms move into the interaction region in the transit relaxation process, $\delta(i,j)$ is the Dirac delta symbol, and N_{ij} describes the relative rate of the elastic interaction of atoms with the walls of the ETC:

$$N_{ij} = \frac{\Delta^2_{col}}{\Delta^2_{col} + |\omega_{ij}|^2}. \tag{12}$$

F. Model for elastic collisions

When atoms move through the cell, they may experience elastic and inelastic interactions with the walls of the ETC. As was shown in [1], the ETC provides the possibility to explore the long-range atom-surface van der Waals interaction and modification of atomic dielectric resonant coupling under the influence of coupling between two neighboring dielectric media, and even the possible modification of interatomic collision processes under the effect of confinement. In addition, if an atom is flying very close to the surface, it can even experience the periodic potential coming from the crystalline surface of the ETC. We will speak about these effects as the effects of elastic collisions occurring with the rate Γ_{col}.

We assume the following model for elastic collisions. First, these collisions do not affect the ground state [Eq. (10)], as in the ground state $L_g=0$, and we assume that these collisions cannot turn the spin—neither the electronic spin S, nor the nuclear spin I. Thus, the collisions affect the excited-state Zeeman coherences and populations [Eq. (11)], as well as the optical coherences described by Eqs. (6) and (7).

The second assumption is that elastic collisions redistribute populations only among excited-state magnetic sublevels [see Eq. (11)], which means that both the optical coherences and the excited-state Zeeman coherences are destroyed completely with the rate Γ_{col}.

Finally, we want to note that the external **B** field not only causes magnetic sublevel splitting $\omega_{e_i e_j}$ and $\omega_{g_i g_j}$, but also alters the dipole transition matrix elements by mixing the hfs levels with the same magnetic quantum number m and with different hfs level angular momentum quantum number F,

$$|e_i\rangle = \sum_{F_e} c^{(e)}_i |F_e m_i\rangle, \tag{13}$$

$$|g_i\rangle = \sum_{F_g} c^{(g)}_i |F_g m_i\rangle. \tag{14}$$

The numerical values of the magnetic sublevel splitting energies $\omega_{e_i e_j}$ and $\omega_{g_i g_j}$, as well as the hf state mixing coefficients $c^{(e)}_i$ and $c^{(g)}_i$, are obtained by diagonalization of the magnetic field interaction Hamiltonian $\widehat{H_B}$, Eq. (2).

The third assumption is the phenomenological model for the redistribution of the excited-state population due to collisions, namely, Eq. (12). The quantity $\Sigma_{e_m} N_{e_k e_m}$ in Eq. (11) is the normalization coefficient. As can be seen from Eq. (12), we assume that the distribution of the probability for the atomic interaction with the ETC walls to mix the populations in the excited state of the atoms has a Lorentzian shape with FWHM Δ_{col}. Thus Δ_{col} could be called the effective width of the elastic collisions.

VII. COMPARISON BETWEEN THEORETICAL AND EXPERIMENTAL RESULTS

Based on the model developed for the ETC, the magneto-optical resonance profiles have been computed for laser frequency detuning over all hfs transitions and for both types of excitation, namely, by linearly and circularly polarized light. In the calculations, the following parameters related to the experimental conditions have been used: $\Gamma=6$ MHz, $\gamma=5$ MHz, $\Delta\omega=3$ MHz, $\Gamma_{col}=200$ MHz, $\Delta_{col}=50$ MHz.

In all the cases considered, the theoretical results are at least in qualitative agreement with the experimental observations. As in the experiment, reduced absorption magneto-optical resonances are predicted by the theory for all $F_g \rightarrow F_e = F_g - 1, F_g$ transitions.

The inclusion in the theoretical model of the influence of the cell walls on the polarization of the excited atomic level has as a result the sign reversal of the bright magneto-optical resonance. Mixing of the excited-state Zeeman sublevels according to Eqs. (11) and (12) is assumed, which for the $F_g \rightarrow F_e = F_g + 1$ transitions results in atomic accumulation in the

ground-state Zeeman sublevels with the lowest probability of excitation (at $\mathbf{B}=\mathbf{0}$). This atomic accumulation in the less favored ground sublevel is the reason for the bright magneto-optical resonance sign reversal. The experimentally observed reduced-absorption magneto-optical resonances at this type of transition support our theoretical result. We would like to remind the reader that, in the case of the $F_g \rightarrow F_e = F_g + 1$ transitions, without the cell window influence, atomic excitation by light of any polarization would result in atomic accumulation in the ground-state Zeeman sublevel with the highest probability of excitation (at $\mathbf{B}=\mathbf{0}$), and hence in the observation of enhanced-absorption, bright magneto-optical resonance.

Let us discuss the behavior of particular magneto-optical resonances when the laser frequency is tuned to the central frequencies of the different hfs transitions. In an interval of a few tens of megahertz around the $F_g=3 \rightarrow F_e=2$ transition, a dark resonance is experimentally observed and is shown in Fig. 9 together with the theoretically simulated profile of the resonance. Here, Cs atoms are irradiated by linearly polarized light and the magnetic field is orthogonal to the polarization vector and to the light propagation direction. A good quantitative agreement between the theoretical and the experimental results can be seen. The resonance amplitude increases with the light power density, and here the agreement of the theory with the experiment is very good. Some discrepancy still remains between the theoretical and experimental resonance widths for low laser power, which can be due to the residual Doppler broadening not accounted for in the model. When the laser power is increased, the transition saturation effects start to dominate over the Doppler broadening. The $F_g=3 \rightarrow F_e=3$ transition behaves similarly to the $F_g=3 \rightarrow F_e=2$ transition. Here also a dark magneto-optical resonance is observed, and also the theoretical profile parameters are in agreement with those of the experimental profiles.

It should be pointed out that the magneto-optical resonance width in the ETC is an order of magnitude larger than that obtained in the ordinary cell. This broadening can be attributed to the larger value of the transit relaxation rate due to the nanometric scale of the ETC thickness as compared to the centimeter dimensions of the ordinary cell. Note that the ETC is not shielded against the laboratory magnetic field because of technical reasons connected with its shape and because the magnetic field must be scanned in quite a large interval. But since $B_{\mathrm{str}} \sim 0.5$ G, the lack of shielding should not significantly influence the resonance width. Moreover, an experiment with an unshielded ordinary cell situated very close to the ETC shows a magneto-optical resonance with less than 1 G width, which proves that the laboratory magnetic field cannot be the main reason for the resonance broadening.

The $F_g=3 \rightarrow F_e=4$ transition represents an interesting case. As mentioned above for the case of the ordinary cell, because of the strong overlapping of the Doppler profiles of the hfs transitions and the low probability of the $F_g=3 \rightarrow F_e=4$ open transition, when tuning the laser frequency in resonance with this transition, it has not been possible to observe enhanced-absorption, (bright) magneto-optical resonances. In the ETC, however, a large-amplitude magneto-optical resonance is observed when the laser frequency is tuned to the center of the transition. But instead of a bright resonance, a dark resonance appears at the $F_g=3 \rightarrow F_e=4$ transition, in agreement with the theoretical model. Both the theoretical and experimental resonance profiles are illustrated in Fig. 10 for irradiation by linearly polarized light. Here also the magnetic field **B** is oriented in a direction orthogonal to the light polarization and to the propagation direction. In the case of this resonance, the theory is also in very good quantitative agreement with the experiment related to the dependence of the resonance amplitude on the laser power density. Here, in the magneto-optical resonance width, a discrepancy between the theory and the experiment is observed

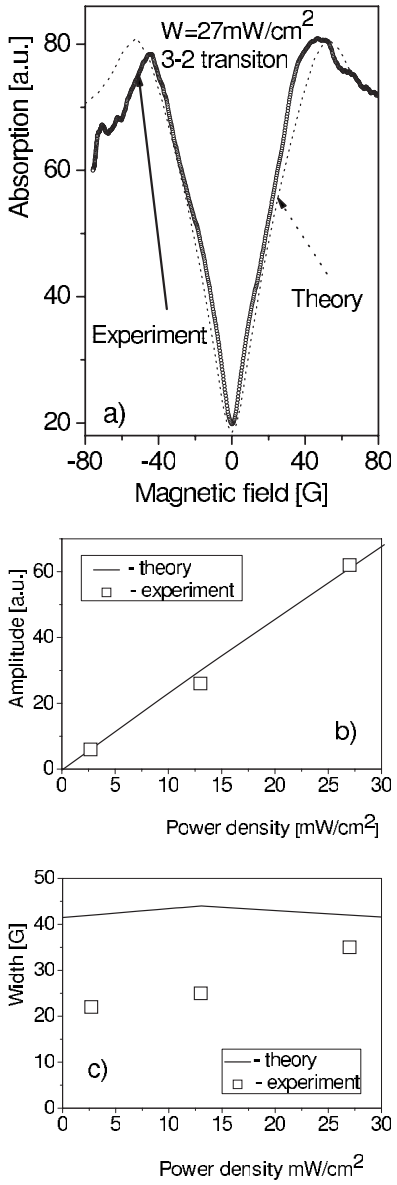

FIG. 9. Comparison between theory and experiment, for $F_g=3 \rightarrow F_e=2$ transition and excitation by linearly polarized light: (a) magneto-optical resonance experimental and theoretical profiles; (b) magneto-optical resonance amplitude as a function of the light power density; (c) magneto-optical resonance width as a function of power density.

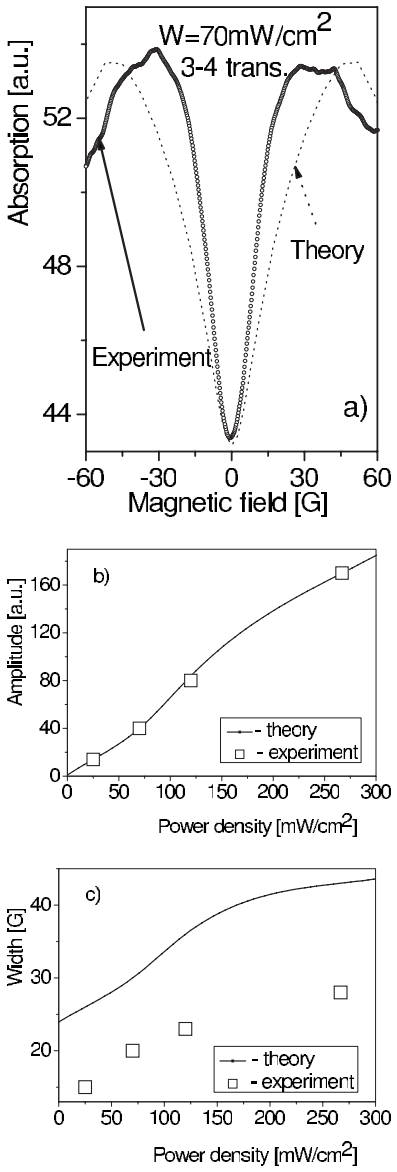

FIG. 10. Comparison between theory and experiment, for $F_g=3\rightarrow F_e=4$ transition and excitation by linearly polarized light: (a) magneto-optical resonance experimental and theoretical profiles; (b) magneto-optical resonance amplitude as a function of light power density; (c) magneto-optical resonance width as a function of power density.

that is even larger than in the previous case. The experimentally observed resonance is significantly narrower than the theoretical one. The origin of this discrepancy can be attributed to the fact that the $F_g=3\rightarrow F_e=4$ transition is an open transition. Therefore, a significant population loss occurs from the $F_g=3$ level to the $F_g=4$ level as a result of the optical pumping through spontaneous transitions from the $F_e=4$ level. In [24–26], it has been shown that, in the case of open transitions, a significant coherent resonance narrowing takes place, because the resonance destruction is more effective at the wings, while at the center the resonance is more resistant to the loss.

Based on the results presented in Fig. 10, we can conclude that, unlike the dark magneto-optical resonance, the bright resonance is very sensitive not only to the depolarization collisions of alkali-metal atoms with those of the buffer gas in the ordinary cell, but also to the surface-atom interactions, about which it can provide valuable information.

In order to confirm the sensitivity of the $F_g\rightarrow F_e=F_g+1$ type of transition to the depolarizing influence of the ETC windows, the behavior of the closed and high-probability $F_g=4\rightarrow F_e=5$ transition is investigated in detail by irradiating Cs atoms with linearly or circularly polarized light. In the first case the scanned magnetic field is oriented orthogonally to the atomic alignment, while in the second case it is orthogonal to the orientation of the atoms. In both cases reduced-absorption magneto-optical resonance is observed experimentally. Expanding the discussion related to Fig. 8, it can be pointed out that, in the case of dilute atoms confined in the ordinary cell and $\mathbf{B}=\mathbf{0}$, irradiation by linearly polarized light also results in atomic accumulation in the ground-state Zeeman sublevels with the highest excitation probabilities. Similarly, also in the case of linear polarization the excited-state depolarization by alkali-metal atom collisions with buffer gas atoms results in a sign reversal of the magneto-optical resonance.

The results obtained from studies with both polarization excitations and with the laser frequency tuned to the central frequency of the $F_g=4\rightarrow F_e=5$ transition confirm the assumed analogy between the excited-state depolarization by atomic collisions (for the ordinary cell) and its depolarization by the influence of the electrical potential of the ETC window. In Fig. 11, a comparison between the experimental and theoretical results is presented for the $F_g=4\rightarrow F_e=5$ transition, in the case of Cs atoms irradiated by circularly polarized light with magnetic field $\mathbf{B}$ applied in a direction orthogonal to the light propagation. It can be seen that in relation to the magneto-optical resonance width, the agreement between the theory and the experiment is better for the $F_g=4\rightarrow F_e=5$ transition. The reason for this can be the fact that, unlike the $F_g=3\rightarrow F_e=4$ transition, the $F_g=4\rightarrow F_e=5$ transition is a closed one, and so the resonance narrowing due to the population loss is not expected. From Figs. 10 and 11 it can be seen that the resonance amplitude at the closed transition increases faster with power than that at the open one, but at the expense of faster broadening of the resonance profile. Note the deviations of the dependences shown in Figs. 10(b), 10(c), 11(b), and 11(c) from linear, which can be expected due to the specific interaction of atoms with the walls (that reverses even the sign of the magneto-optical resonance) and due to the different dynamics of contributions of atoms depending on their velocities and the light intensity.

VIII. CONCLUSION

We have presented an experimental and theoretical study of the ground-state magneto-optical resonances observed in Hanle configuration on the D_2 line of Cs. In a centimeter-scale ordinary cell containing Cs vapor, the optical hyperfine transitions starting from a single ground-state level are strongly overlapped, which is a reason for the mixing of the contribution of different hfs transitions that are responsible for the dark and bright magneto-optical resonances. It is

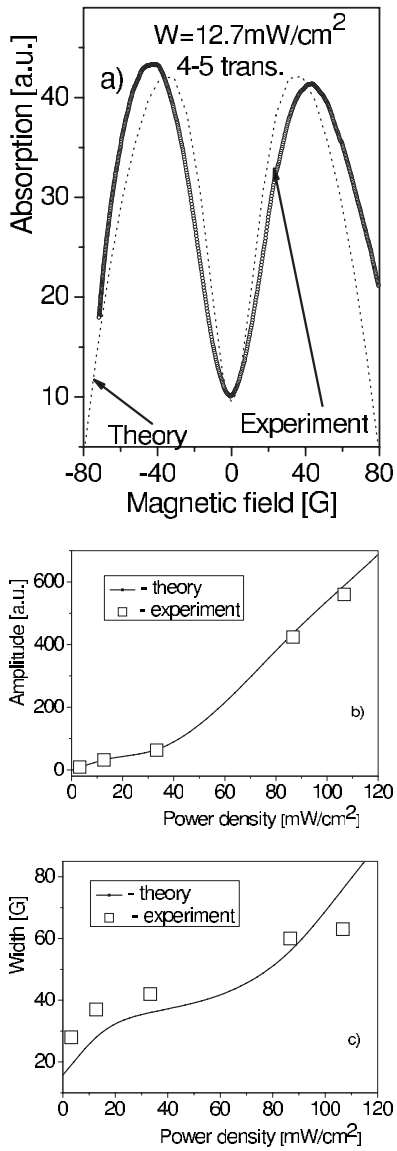

FIG. 11. Comparison between theory and experiment, for $F_g=4\rightarrow F_e=5$ transition and excitation by circularly polarized light: (a) magneto-optical resonance experimental and theoretical profiles; (b) magneto-optical resonance amplitude as a function of light power density; (c) magneto-optical resonance width as a function of power density.

shown that the utilization of an extremely thin cell with thickness equal to the wavelength of the irradiating light allows one to examine the formation of a magneto-optical resonance on the individual hfs transitions due to the experimentally proven fact that only very slow atoms possess enough interaction time with the light to form the magneto-optical resonance. The fast atoms, mainly exhibiting a single act of absorption during their interaction with the light, do not contribute to the magneto-optical resonance formation.

It is shown that in the ETC, dark (reduced absorption) magneto-optical resonances are observed at $F_g\rightarrow F_e=F_g-1$, F_g transitions, much like in ordinary cells. However, in the case of the $F_g\rightarrow F_e=F_g+1$ transitions, Cs atoms confined in ETC exhibit completely different behavior as compared to those contained in an ordinary cell. For the latter, bright (enhanced absorption) magneto-optical resonances have been observed in dilute Cs vapor. As a result of our study, we report on the bright resonance sign reversal in Cs atoms confined in the ETC. Both ($F_g=3\rightarrow F_e=4$ and $F_g=4\rightarrow F_e=5$) intrinsically bright transitions are responsible for dark magneto-optical resonance formation in the ETC.

A theoretical model is proposed based on the optical Bloch equations that incorporates the elastic interaction processes of atoms with ETC walls. The assumed elastic collisions of Cs atoms with the cell walls do not affect the ground state of alkali-metal atoms and do not reorient the electronic and nuclear spins of the atom, but do affect the excited-state Zeeman coherences and populations, as well as the optical coherences. The involvement of elastic collisions of this type results in depolarization of the Cs excited state that had been polarized by the exciting radiation. This depolarization leads to the accumulation of atomic population in ground-state Zeeman sublevels with the lowest probability of excitation. This is opposite to the situation in the ordinary cell, where atoms accumulate on the Zeeman sublevel possessing the largest probability of excitation. Hence, the influence of the ETC wall on the atomic polarization leads to the sign reversal of the bright resonance. Using the proposed model, the magneto-optical resonance amplitude and width dependences on laser power are calculated and compared with the experimental ones. The numerical results are in good agreement with the experiment.

The obtained results show that the magneto-optical resonances observed in the ETC could potentially be applied to study atom-surface interactions. Further investigations are needed for clarification of the physical reason behind the elastic collision process.

ACKNOWLEDGMENTS

The authors are grateful to Professor D. Sarkisyan for providing the ETC and for a number of extremely useful discussions. We thank Dr. F. Gahbauer for the careful reading of the manuscript. We also acknowledge partial support from the INTAS program (Grant No. 06-1000017-9001). C.A., S.C., L.P., and D.S. acknowledge support from the Bulgarian Fund for Scientific Research (Grant No. F-1404/04). A.A., M.A., and K.B. acknowledge support from EU FP6 TOK project LAMOL and European Regional Development Fund Project No. 2.5.1./000035/018. A.A. and K.B. gratefully acknowledge support from the European Social Fund. S.C. appreciates the very helpful discussions with Professor D. Bloch, Professor M. Ducloy, and Professor Yu. Malakyan related to the particular properties of the atoms confined in the ETC and magneto-optical resonances.

[1] I. Hamdi, P. Todorov, A. Yarovitski, G. Dutier, I. Maurin, S. Saltiel, Y. Li, A. Lezama, T. Varzhapetyan, D. Sarkisyan, M.-P. Gorza, M. Fichet, D. Bloch, and M. Ducloy, Laser Phys. **15**, 987 (2005).
[2] D. Sarkisyan, D. Bloch, A. Papoyan, and M. Ducloy, Opt. Commun. **200**, 201 (2001).
[3] D. Sarkisyan, T. Becker, A. Papoyan, P. Theumany, and H. Walter, Appl. Phys. B: Lasers Opt. **76**, 625 (2003).
[4] G. Dutier, A. Yarovitski, S. Saltiel, A. Papoyan, D. Sarkisyan, D. Bloch, and M. Ducloy, Europhys. Lett. **63**, 35 (2003).
[5] R. H. Romer and R. H. Dicke, Phys. Rev. **99**, 532 (1955).
[6] D. Sarkisyan, T. Varzhapetyan, A. Sarkisyan, Yu. Malakyan, A. Papoyan, A. Lezama, D. Bloch, and M. Ducloy, Phys. Rev. A **69**, 065802 (2004).
[7] Y. Dancheva, G. Alzetta, S. Cartaleva, M. Taslakov, and Ch. Andreeva, Opt. Commun. **178**, 103 (2000).
[8] F. Renzoni, C. Zimmermann, P. Verkerk, and E. Arimondo, J. Opt. B: Quantum Semiclassical Opt. **3**, S7 (2001).
[9] A. Papoyan, M. Auzinsh, and K. Bergmann, Eur. Phys. J. D **21**, 63 (2002).
[10] J. Alnis, K. Blushs, M. Auzinsh, S. Kennedy, N. Shafer-Ray, and E. R. I. Abraham, J. Phys. B **36**, 1161 (2003).
[11] J. Alnis and M. Auzinsh, J. Phys. B **34**, 3889 (2001).
[12] C. Andreeva, S. Cartaleva, Y. Dancheva, V. Biancalana, A. Burchianti, C. Marinelli, E. Mariotti, L. Moi, and K. Nasyrov, Phys. Rev. A **66**, 012502 (2002).
[13] I. Maurin, P. Todorov, I. Hamdi, A. Yarovitski, G. Dutier, D. Sarkisyan, S. Saltiel, M.-P. Gorza, M. Fichet, D. Bloch, and M. Ducloy, J. Phys.: Conf. Ser. **19**, 20 (2005).
[14] S. Briaudeau, D. Bloch, and M. Ducloy, Phys. Rev. A **59**, 3723 (1999).
[15] D. V. Brazhnikov, A. M. Tumaikin, V. I. Yudin, and A. V. Taichenachev, J. Opt. Soc. Am. B **22**, 57 (2005).
[16] D. V. Brazhnikov, A. V. Taichenachev, A. M. Tumaikin, V. I. Yudin, S. A. Zibrov, Ya. O. Dudin, V. V. Vasil'ev, and V. L. Velichansky, JETP Lett. **83**, 64 (2006).
[17] S. Stenholm, *Foundations of Laser Spectroscopy* (Dover, Mineola, NY, 2005).
[18] M. Auzinsh and R. Ferber, *Optical Polarization of Molecules* (Cambridge University Press, Cambridge, UK, 2005).
[19] D. A. Varshalovich, A. N. Moskalev, and V. K. Khersonskii, *Quantum Theory of Angular Momentum* (World Scientific, Singapore, 1988).
[20] R. N. Zare, *Angular Momentum, Understanding Spatial Aspects in Chemistry and Physics* (Wiley, New York, 1988).
[21] L. Allen and J. H. Eberly, *Optical Resonance and Two Level Atoms* (Wiley, New York, 1975).
[22] N. G. van Kampen, Phys. Rep., Phys. Lett. **24**, 171 (1976).
[23] K. Blush and M. Auzinsh, Phys. Rev. A **69**, 063806 (2004).
[24] F. Renzoni and E. Arimondo, Europhys. Lett. **46**, 716 (1999).
[25] F. Renzoni, A. Lindner, and E. Arimondo, Phys. Rev. A **60**, 450 (1999).
[26] F. Renzoni and E. Arimondo, Phys. Rev. A **58**, 4717 (1998).